DOI 10.5012/bkcs.2010.31.10.2877

Folding Mechanism of WT* Ubiquitin Variant Studied by Stopped-flow Fluorescence Spectroscopy

Soon-Ho Park

Department of Biochemistry and Molecular Biology, Research Institute of Oral Sciences, College of Dentistry, Gangneung-Wonju National University, Gangneung 210-702, Korea. E-mail: spark9@gwnu.ac.kr
Received July 21, 2010, Accepted August 23, 2010

The folding kinetics of WT* ubiquitin variant with valine to alanine mutation at sequence position 26 (HubWA) was studied by stopped-flow fluorescence spectroscopy. While unfolding kinetics showed a single exponential phase, refolding reaction showed three exponential phases. The semi-logarithmic plot of urea concentration *vs.* rate constant for the first phase showed v-shape pattern while the second phase showed v-shape with roll-over effect at low urea concentration. The rate constant and the amplitude of the third phase were constant throughout the urea concentrations, suggesting that this phase represents parallel process due to the configurational isomerization. Interestingly, the first and second phases appeared to be coupled since the amplitude of the second phase increased at the expense of the amplitude of the first phase in increasing urea concentrations. This observation together with the roll-over effect in the second folding phase indicates the presence of intermediate state during the folding reaction of HubWA. Quantitative analysis of HubWA folding kinetics indicated that this intermediate state is on the folding pathway. Folding kinetics measurement of a mutant HubWA with hydrophobic core residue mutation, Val to Ala at residue position 17, suggested that the intermediate state has significant amount of native interactions, supporting the interpretation that the intermediate is on the folding pathway. It is considered that HubWA is a useful model protein to study the contribution of residues to protein folding process using folding kinetics measurements in conjunction with protein engineering.

Key Words: Protein folding kinetics, Folding intermediate, Native interaction

Introduction

Protein folding process has been studied by measuring folding kinetics in conjunction with protein engineering.[1-4] This method measures the effect of a mutation on the stability of the native state and the folding transition state. Through these measurements, the contribution of a residue to the folding reaction was investigated. This method has been applied to several small globular proteins and provided the information useful to understand the protein folding process.[5-13] Since wild type protein is the mutational background for these studies, a thorough elucidation of folding mechanism of the wild type protein should be done prior to mutational study.

Ubiquitin with tryptophan substitution for phenylalanine at sequence position 45, the pseudo-wild type ubiquitin (WT* ubiquitin),[14] has been widely used as a model protein to study protein folding, stability, design, *etc.*[15] This tryptophan provided a fluorescence probe for folding study. Although the folding kinetics study of WT* ubiquitin has been carried out by several groups, the folding mechanism determined by these studies has been controversial. The first folding kinetics study of WT* ubiquitin showed missing amplitude (burst phase) in the 2 ms dead-time of the stopped-flow device.[16] Furthermore, the rate profile (denaturant concentration *vs.* rate constant in a log scale) was observed to be curved at low concentrations of denaturant (roll-over effect). Normally the rate profile was observed to be v-shaped linear pattern for a two-state folding mechanism. The curved pattern in the low denaturant concentrations, a roll-over effect, was interpreted as a presence of one or more states except the native and unfolded state during the folding reaction.[5] Khorasanizadeh *et al.* interpreted that the burst phase and the roll-over effect represented a presence of folding intermediate in the sub-ms time scale. Through quantitative kinetic modeling, they concluded that this burst phase intermediate was an on-pathway intermediate with near native-like compactness. They found that this burst phase intermediate was stabilized mainly by hydrophobic interactions. However, later folding kinetics study of WT* ubiquitin by Sosnick and coworkers showed no burst phase and roll-over effect.[17] They concluded that WT* ubiquitin fold by a two-state mechanism. They argued that the burst phase and roll-over effect would be an experimental artifact since the rate constant and amplitude of a very fast reaction whose time constant is close to the dead-time of the stopped-flow device is very difficult to resolve. Yet another folding kinetics study of WT* ubiquitin by Jackson and coworkers showed the conspicuous roll-over effect in the refolding reaction at low denaturant concentrations.[18] They interpreted that this roll-over effect is due to the transient aggregation in the hydrophobic collapsed state at the dead-time of the stopped-flow device, since they observed the retardation of folding rate as the protein concentration was increased. This concentration dependence is usually interpreted as the occurrence of transient aggregation in the early folding time.[19] Since the transiently aggregated state should be an off-pathway intermediate, the folding reaction should be delayed until the transiently aggregated intermediate unfolds and resumes folding reaction, which results in the retardation of folding rate.

To broaden our understanding of protein folding pathway by measuring folding kinetics in conjunction with protein engineering, we decide to use variant WT* ubiquitin with Val 26 to Ala substitution (V26A WT* ubiquitin) as a mutational background. Here after V26A WT* ubiquitin is referred to as HubWA. As shown in Fig. 1, Val 26 is located in the hydro-

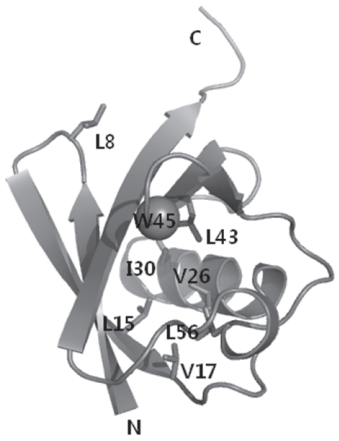

Figure 1. Ribbon diagram of human ubiquitin illustrating the core region near Val 26. The side chain of Val 26 and the side-chains of core residues contact with Val 26 are shown as stick. The α-carbon of Trp 45 is shown as a sphere. The side-chain of Leu8 is also shown as stick.

phobic core of WT* ubiquitin. The mutation of valine to a less hydrophobic alanine has been shown to decrease the stability of the native state significantly.[16] Thus, it was expected that the destabilization of hydrophobic core may allow us to avoid the controversial observations such as burst phase intermediate or transient aggregation, *etc*, in the early folding time since all these phenomena were considered to be originated from hydrophobic interactions. It was expected that HubWA may reduce to a simpler folding mechanism so that the mutational effect can be resolved and interpreted unambiguously.

Materials and Methods

Materials. The plasmid pNMHUB containing WT* ubiquitin gene was provided by Heinrich Roder (Fox Chase Cancer Center, USA). WT* ubiquitin gene was subcloned into pET-30b vector purchased from Novagen (USA) and named as pET-Hub. After construction of pET-Hub, valine at sequence position 26 was mutated to alanine and named as pET-HubWA. Mutagenesis of Leu 8 to Ala and Val 17 to Ala was done by using pET-HubWA plasmid as a template. Site-directed mutagenesis was carried out by using QuikChange Site-directed Mutagenesis Kit from Stratagene (USA). DNA oligomers for site-directed mutagenesis were purchased from Genotech (Korea). Mutations were confirmed by DNA sequencing. HubWA and mutant proteins were expressed in *E. coli* strain BL21(DE3) using isopropyl β-D-1-thiogalactopyranoside (IPTG). HubWA and mutants were purified by previously described method with some modifications.[14,20] Since HubWA and mutants were considered to be less stable than the WT* ubiquitin, heating the cell lysate at 85 °C for 5 min was omitted to improve the yield. The Q-sepharose Fast Flow column chromatography was replaced by DEAE-sephacel column chromatography. DEAE-sephacel fractions containing HubWA or mutants were further purified by sephacryl S-100 column chromatography. The collected fractions of sephacryl S-100 column chromatography were dialyzed against deionized water and then lyophilized extensively. The dried HubWA and mutants were stored at −70 °C until use. The purified proteins were detected as a single band in overloaded electrophoresis gels stained by coommassie brilliant blue. Ultrapure urea was purchased from ICN Biomedicals Inc (USA). All other chemicals were reagent grade or better.

Folding kinetics measurements. Time course of refolding and unfolding reactions of HubWA and mutants in various urea concentrations was measured by monitoring the changes in the intrinsic tryptophan fluorescence emission as a function of time. All measurements were made using a BioLogic SFM-4 stopped-flow device in fluorescence mode. Refolding kinetics were measured by 1:10 dilution of unfolded proteins in 6 M urea solution with buffer (25 mM acetate, pH 5) containing 1~3 M urea to generate folding conditions in various final urea concentrations. Urea solutions were placed in the syringes 1 to 3 and the solution containing unfolded protein was placed in the syringe 4. Unfolding kinetics were measured by 1:10 dilution of native protein in buffer (25 mM acetate, pH 5) with solutions containing 3 ~ 6 M urea to generate unfolding conditions in various final urea concentrations. Urea solutions were placed in the syringes 1 to 3 and the solution containing the native protein was placed in the syringe 4. The final concentration of proteins in urea dependent folding kinetics measurement was ~3 μM. For concentration dependent folding kinetics study, protein concentrations were increased from 0.28 to 28 μM. The tryptophan side-chain was excited at 295 nm and the change in fluorescence emission above 324 nm was measured using a 324 nm cut-off filter. All the stopped-flow kinetics measurements were made at 25 °C. The dead-time of the stopped-flow device was measured to be 4 ms using the method described by Peterman.[21] For the analysis of kinetic traces, at least five traces were averaged for each refolding or unfolding reaction. The averaged traces were fitted to a single exponential equation for unfolding kinetic traces, and three exponential equations for refolding kinetic traces with nonlinear least squares method. The quality of fit was judged by analyzing fitting residuals.

Analysis of folding kinetics. Folding kinetic data of HubWA and mutants were fitted to a three-state mechanism shown as on-pathway model (Scheme 1) or off-pathway model (Scheme 2).[22] In these schemes N, I, and U represent the native, intermediate, and unfolded states, respectively.

$$\mathrm{U} \underset{k_{IU}}{\overset{k_{UI}}{\rightleftharpoons}} \mathrm{I} \underset{k_{UN}}{\overset{k_{IN}}{\rightleftharpoons}} \mathrm{N}$$

Scheme 1

$$\mathrm{I} \underset{k_{UI}}{\overset{k_{UI}}{\rightleftharpoons}} \mathrm{U} \underset{k_{NU}}{\overset{k_{IN}}{\rightleftharpoons}} \mathrm{N}$$

Scheme 2

Each elementary reaction in a three-state model is considered to be a reversible two-state process with microscopic rate constants, k_{IJ}. Thus the rate constants of forward and backward reactions for U⇌I elementary reaction are k_{UI} and k_{IU}, respectively. It has been observed that the logarithm of the microscopic rate constant of elementary reaction is linearly dependent on urea

concentration as in equation 1:[23-25]

$$\ln k_{IJ} = \ln k_{IJ}^{o} + (m_{IJ}^{\ddagger}/RT)C \quad (1)$$

where k_{IJ}^{o} represents the microscopic rate constant at 0 M urea, C denotes the concentration of urea, and $m_{IJ}^{\ddagger}/RT$ represents the slope of $\ln k_{IJ}$ *vs*. C. R is gas constant and T is absolute temperature. Observable rate constants and fractional amplitude were calculated by solving the analytical solutions to the rate matrix for a three-state reaction.[22] Calculations were performed on a personal computer using Excel (Microsoft, USA) and the comparison of calculated value and observed data was done by using SigmaPlot (Systat, USA).

Results and Discussion

The controversies in folding mechanism of WT* ubiquitin was due mainly to the hydrophobic collapsed state occurred in the dead-time (~2 ms) of stopped-flow device. This state was interpreted as a burst phase intermediate or transiently aggregated intermediate.[16,18] We studied the folding kinetics of a mutant WT* ubiquitin with less stable hydrophobic core. Previously, it has been shown that the mutation of the hydrophobic core residue Val 26 to Ala (HubWA) significantly destabilized the native state.[16] It was expected that HubWA folding may not be complicated with either burst phase or transient aggregation since the mutation was considered to destabilize the hydrophobic collapsed state. Furthermore, destabilization of the native state for this mutant ubiquitin may allow using the urea as a denaturant. Although urea is less strong denaturant than guanidinium chloride, it has been recommended that neutral urea is better than ionic guanidinium chloride as a denaturant for folding study.[26]

Fig. 2A shows the refolding kinetic trace of HubWA refolding at 0.6 M final urea concentration. The refolding kinetic trace was fitted with three exponential equations. The extrapolated signal at time zero is nearly same as the expected signal (arrow in Fig. 2A) for unfolded state at 0.6 M urea concentration (see upper dotted line in Fig. 4B). This observation indicates that there is no observable missing amplitude (burst phase) in refolding of HubWA at the dead-time of stopped-flow device. Fig. 2B shows the rate constants of three exponential phases of HubWA refolding in varying protein concentrations at the same final urea concentration as in Fig. 2A. Previously, transient aggregation significantly retarded the WT* ubiquitin folding rates when protein concentration was increased from ~1 μM to ~5 μM.[18] As shown in Fig. 2B, no retardation of folding rate was observed at the protein concentrations between 0.28 μM and 28 μM. The independence of folding rate constants to protein concentrations suggests that no transient aggregation occurs in the HubWA refolding reaction. Based on these observations, it is considered that the folding reaction of HubWA is not complicated by formation of burst phase intermediate or transient aggregate at the early folding time. It is thought that HubWA would be a useful model protein to be used as a mutational background for folding kinetics study in conjunction with protein engineering.

Fig. 3A shows a representative refolding kinetic trace of HubWA at 3.25 M urea concentration. Judged by the fitting residuals as shown in Fig. 3B, 3C, and 3D, three exponential equations provide the best fit of the kinetic trace. The unfolding kinetic trace of HubWA showed a single exponential phase consistent with previous measurements.[14,17] Semi-logarithmic plot of the refolding and unfolding rate constants of HubWA as a function of urea concentrations are shown in Fig. 4A. The corresponding amplitudes for each phase and the signal at long time, which corresponds to the signal reached at equilibrium, are shown in Fig. 4B. The first refolding phase shows a typical v-shaped chevron pattern, indicating that this phase represents a conformational folding process.[25] The rate constant of the second phase was decreased as increasing urea concentrations. Interestingly the second phase shows slight roll-over effect at low urea concentrations. The rate constants of unfolding reaction (filled squares in Fig. 4A) appeared to be merged with those of the second refolding phase. The second refolding phase and

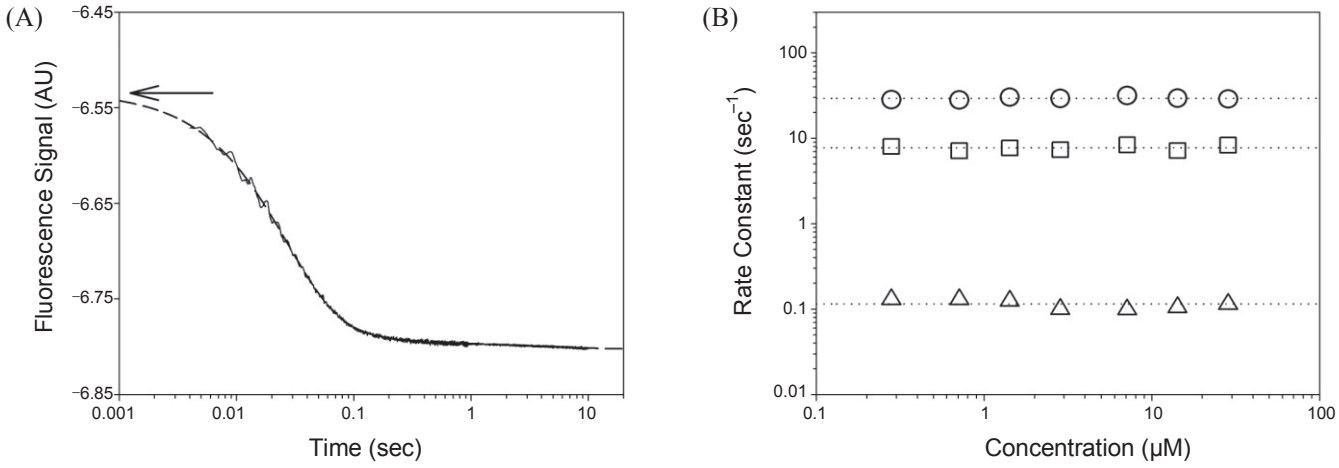

Figure 2. Kinetic trace and concentration dependence of HubWA refolding reaction at final 0.6 M urea concentration. Panel A illustrates the refolding kinetic trace. The long dashed line illustrates the fitting of the observed trace to three exponential equations. The arrow denotes the fluorescence signal at time zero. Panel B illustrates the rate constants of three observed phases of HubWA refolding kinetic trace at final 0.6 M urea concentration in varying HubWA concentrations. Circles, squares, and triangles represent the rate constants of the first, second, and third phase, respectively.

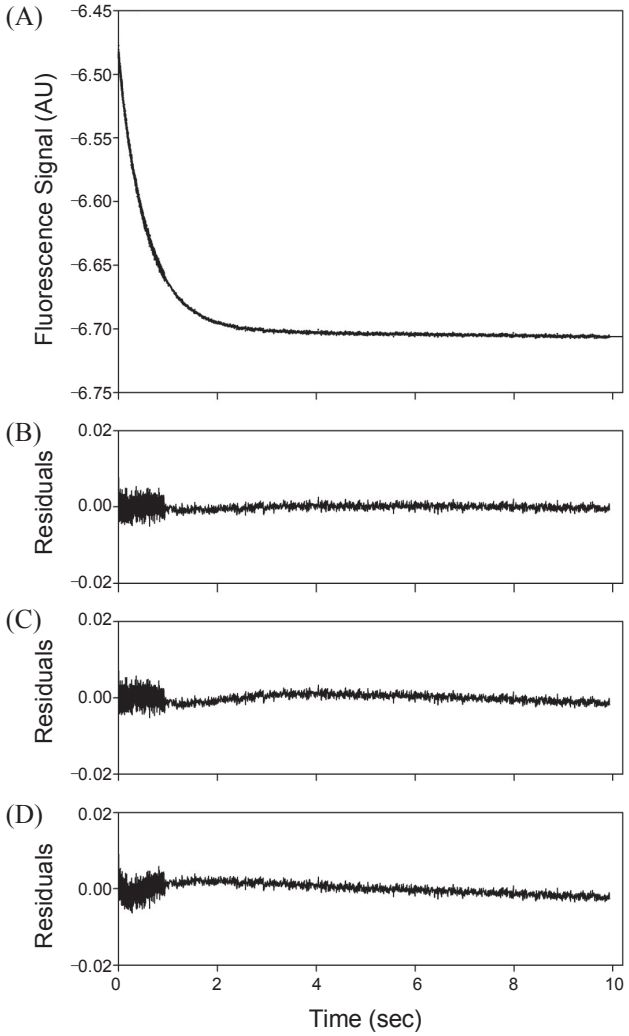

Figure 3. Analysis of representative refolding kinetic trace at final 3.25 M urea concentration. Panel A is the kinetic trace. Panel B, C, and D are residuals of triple, double, and single exponential analysis, respectively.

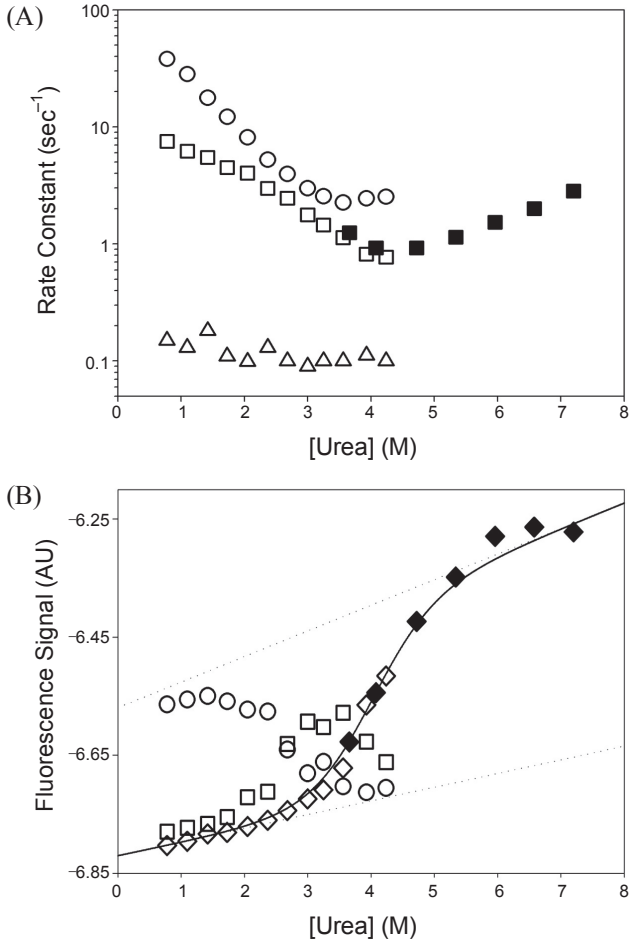

Figure 4. Rate and amplitude profile of HubWA. Rate constants in a log scale are shown as a function of urea concentration in Panel A. Circles, squares, and triangles correspond to the rate constants of the first, second, and the third refolding phases, respectively. Filled squares correspond to the rate constant of unfolding phases. Panel B illustrates the fluorescence signals. Circles and squares are amplitudes of the first and second refolding phases, respectively. Observed amplitude values were added to the native baseline value (lower dotted line) for plotting. Open and closed diamonds are fluorescence signal at long times for refolding and unfolding kinetics measurements, respectively. Solid line represents the unfolding transition curve obtained by equilibrium unfolding experiment.[27]

unfolding phase also formed the v-shaped chevron pattern, indicating that this phase represents another folding process in HubWA folding reaction. The amplitude of the second phase (squares in Fig. 4B) increased at the expense of the amplitude of the first phase (circles in Fig. 4B) between 2 and 3.5 M urea concentrations, suggesting that the first and the second phase are coupled. When urea concentration was further increased, the amplitude of the second phase decreased while the amplitudes of unfolded state increased. The urea dependence of the fluorescence signals at long times (open and closed diamonds in Fig. 4B) is equivalent to equilibrium unfolding measurements and results in nearly same transition curve as observed before, shown as solid line in Fig. 4B.[27] Based on the v-shaped rate profile for both the first and the second phases, roll-over effect of the second phase at low denaturant concentrations, and amplitude changes of the first and the second phase, it is considered that the second phase of HubWA folding reaction represents the presence of folding intermediate.[28] The rate constants, ~0.1 sec^{-1}, and corresponding amplitude, ~ 5% of total amplitude, of the third phase were observed to be constant throughout the urea concentrations. This result is consistent with the folding kinetics of WT* ubiquitin.[14,16,17] It has been interpreted that this phase is due to the *cis/trans* isomerization of Xaa-Pro peptide bond. The folding phase caused by configurational isomerization normally interpreted to represent a parallel folding pathway.[16,17] Thus the third phase is not included in the folding kinetics analysis.

Two coupled exponential phases in folding kinetics and roll-over effect in the second refolding phase suggest that there are three states, the native state, unfolded state and the intermediate state in the folding process of HubWA. The first observable phase is due to the formation of the intermediate state from unfolded state and the second observable phase is due to the formation of the native state. For the reaction with three states,

there are at least three possible reaction pathways, on-pathway model (Scheme 1), off-pathway model (Scheme 2) and triangular model (Scheme 3).

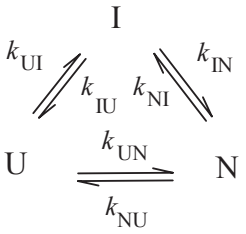

Scheme 3

In the triangular model, it is considered that there are two parallel pathways. One is a direct pathway from unfolded state to the native state, and the other is sequential pathway from unfolded state to the native state *via* intermediate state. The triangular mechanism suggests that there are two conformationally different populations of unfolded species that fold along either of two pathways. The conformational study of ubiquitin unfolded state in 8 M urea at acidic pH indicated no conformationally distinct species.[29] Thus it is unlikely that HubWA, which is different from wild type ubiquitin by only two residues, has conformationally different species in unfolded state. It is not considered that HubWA may fold through triangular folding mechanism. Furthermore, in triangular model, when U to N transition is slower than I to N transition, the reaction mechanism would be reduced to a three-state on-pathway model (Scheme 1), and when U to N transition is faster than I to N transition, the reaction mechanism would be reduced to a three-state off-pathway model (Scheme 2).

The folding kinetics of HubWA was fitted to either on- or off-pathway model to understand the folding mechanism. In the on-pathway model, the intermediate state is on the folding pathway with subset of native interactions. In the off-pathway model, the intermediate state is nonspecifically collapsed state with some non-native interactions that should be unfolded before the native state is formed. The calculated rate constants and normalized signals as a function of urea concentrations are shown as solid lines in Fig 5. It appears that on-pathway model fits the observed folding kinetics reasonably well. In off-pathway model, the calculated rate constants of second phase (λ_2) were severely off the observed rate constant at low concentrations of urea. This is because that in off-pathway model, λ_2 should be smaller than microstate rate constant k_{IU}. Furthermore, the normalized amplitudes were also fitted poorly to the off-pathway model. Based on these analyses, it was concluded that the on-pathway model is more plausible than the off-pathway model for HubWA folding reaction.

The folding reaction of HubWA was further studied using HubWA variants with Leu8 to Ala mutation (HubWA-L8A) and Val17 to Ala mutation (HubWA-V17A). As shown in Fig. 1, Leu8 is located on the loop between strand 1 and 2. The side-chain of Leu8 is exposed to surrounding solvent with virtually no native interactions. On the other hand, the side-chain of Val17 is located in the interior of HubWA forming various native interactions with other hydrophobic core residues. Since

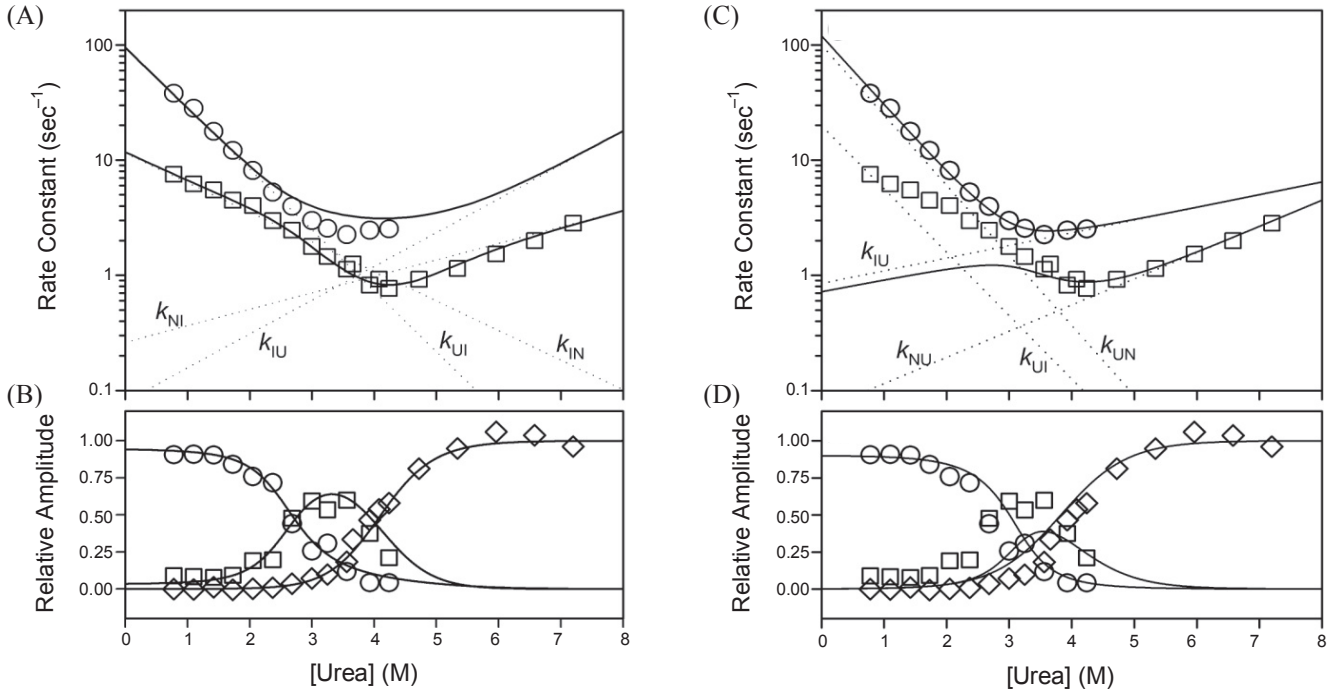

Figure 5. Three state kinetic analysis of HubWA folding reaction. Panel A and B are on-pathway model and Panel C and D are off-pathway model. Circles and squares in Panel A and C represent the rate constants of first and second phases as a function of urea concentrations. Solid lines and dotted lines in Panel A and C are calculated folding rate constants and microstate rate constants, respectively. Circles and squares of Panel B and D represent the normalized amplitudes of first and second phases. Diamonds of Panel B and D are normalized signal at long times. Solid lines in Panel B and D represent the calculate values based on the appropriate model.

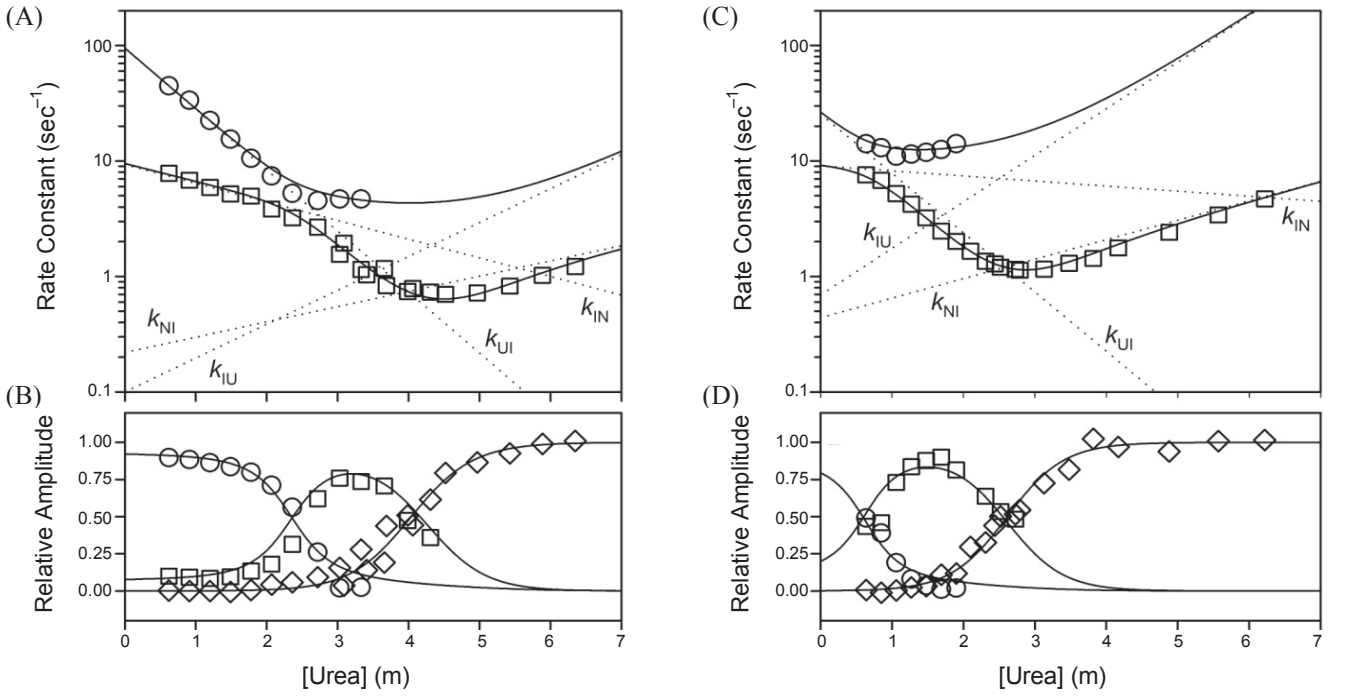

Figure 6. Three state kinetic analysis of HubWA-L8A and HubWA-V17A. Panel A and B illustrate the kinetic analysis of HubWA-L8A and Panel C and D illustrate the kinetic analysis of HubWA-V17A. Circles and squares in Panel A and C represent the rate constants of first and second phases as a function of urea concentrations. Solid lines and dotted lines in Panel A and C are calculated folding rate constants and microstate rate constants, respectively. Circles and squares of Panel B and D represent the normalized amplitudes of first and second phases. Diamonds of Panel B and D are normalized signal at long times. Solid lines in Panel B and D represent the calculate values based on a three-state on-pathway model.

Table 1. Kinetic parameters for the folding and unfolding of HubWA, HubWA-L8A, and HubWA-V17A

Protein	k^o_{UI}	$m^{\ddagger}_{UI}$	k^o_{IU}	$m^{\ddagger}_{IU}$	k^o_{IN}	$m^{\ddagger}_{IN}$	k^o_{NI}	$m^{\ddagger}_{NI}$	ΔG^o_{UI}	ΔG^o_{IN}	ΔG^o_{UN}	β_{TS1}	β_I	β_{TS2}
HubWA	95.0	−0.72	0.08	0.39	11.0	−0.35	0.25	0.20	−4.2	−2.2	−6.4	0.43	0.67	0.88
HubWA-L8A	95.0	−0.72	0.10	0.40	9.3	−0.22	0.22	0.18	−4.1	−2.2	−6.3	0.47	0.74	0.88
HubWA-V17A	25.5	−0.72	0.69	0.40	10.2	−0.19	0.44	0.23	−2.1	−1.9	−4.0	0.47	0.73	0.85

Free energies of folding are calculated as $\Delta G^o_{UI} = -RT ln(k^o_{UI}/k^o_{IU})$, $\Delta G^o_{IN} = -RT ln(k^o_{IN}/k^o_{NI})$, and $\Delta G^o_{UN} = \Delta G^o_{UI} + \Delta G^o_{IN}$. β-values are calculated as $\beta_{TS1} = -m^{\ddagger}_{UI}/m_{eq}$, $\beta_I = (m^{\ddagger}_{IU} - m^{\ddagger}_{UI})/m_{eq}$, and $\beta_{TS2} = (m^{\ddagger}_{IU} - m^{\ddagger}_{UI} - m^{\ddagger}_{IN})/m_{eq}$, where $m_{eq} = m^{\ddagger}_{IU} - m^{\ddagger}_{UI} + m^{\ddagger}_{NI} - m^{\ddagger}_{IN}$.

it is considered that the protein folding process is the progressive formation of the native interactions,[30,31] it is expected that the mutation of Val17 to Ala may affect the folding process of HubWA while the mutation of Leu8 to Ala may not influence the folding process. As shown in Fig. 6 and Table 1, folding kinetics of both HubWA-L8A and HubWA-V17A are fitted to a three-state on-pathway model quite well. In the folding kinetics analysis, the β-value has been interpreted as compactness,[32] hence the degree of folding progression, of variously states occurred during folding reaction. The β-values are defined as the ratio of cumulative m-values relative to equilibrium m-value (m_{eq}) so that $\beta_{TS1} = -m^{\ddagger}_{UI}/m_{eq}$, $\beta_I = (m^{\ddagger}_{IU} - m^{\ddagger}_{UI})/m_{eq}$, and $\beta_{TS2} = (m^{\ddagger}_{IU} - m^{\ddagger}_{UI} - m^{\ddagger}_{IN})/m_{eq}$, where $m_{eq} = m^{\ddagger}_{IU} - m^{\ddagger}_{UI} + m^{\ddagger}_{NI} - m^{\ddagger}_{IN}$. The β-value has the number between 0 (completely unfolded state) and 1 (native state). As listed in Table 1, β-values of the first transition state (β_{TS1}), intermediate state (β_I), and the second transition state (β_{TS2}) for HubWA, HubWA-L8A, and HubWA-V17A are appeared to be fairly similar, suggesting that each state occurred in the folding reaction of these proteins has similar compactness. The burial of solvent accessible surface area for the first transition state, an intermediate state, and the second transition state were ~45%, ~70%, and ~85%, respectively. This observation indicates that the mutation does not affect a three-state folding mechanism of HubWA, HubWA-L8A, and HubWA-V17A. The gradual increase of β-value suggests that HubWA fold through progressively more compact states. Folding kinetics of HubWA-V17A was fitted reasonably well by mainly adjusting k_{UI}^o (~4-fold decrease) and k_{IU}^o (~ 9-fold increase) values as compared to those of HubWA. This effect reflects the ~2.1 kcal/mol decrease in the stability of HubWA-V17A folding intermediate as compared to that of HubWA. Since the destabilization of the native state for Val17 to Ala mutation was ~2.5 kcal/mol, it could be considered that a significant amount of native interactions are contributed to the stability of the intermediate state. The fitting parameters of HubWA-L8A are nearly same as those of HubWA, suggesting that the Leu8 is not involved in overall folding reaction. These observations support the conclusion that the HubWA folding intermediate, which appeared to have signi-

ficant amount of native interactions, is on the folding pathway. Furthermore, the analysis of Val17 to Ala mutant folding kinetics result suggests that the effect of residues on the folding reaction of HubWA might be investigated by judicious replacements of residues involved in the native interactions. Previously it was observed that HubWA formed denatured state with some native-like conformational properties in strong acidic and basic solutions.[27] The denatured state in basic solution observed to have equilibrium m-value which is equivalent to ~55% burial of solvent accessible surface area. Although the denatured state in the basic solution appeared to be less compact than the kinetic intermediate in this study, it might be interesting to compare the conformational properties of kinetic intermediate and equilibrium denatured state.

Folding kinetics study of variant WT* ubiquitin, HubWA, would be summarized as follow. HubWA was shown to be a better model for studying the folding process than WT* ubiquitin since the controversial aspects of WT* ubiquitin folding reaction, such as the burst phase and the transient aggregation, were not observed in the dead-time of stopped-flow device. The folding kinetics analysis of HubWA indicated that HubWA folds through a three-state on-pathway mechanism (Scheme 1). Since the overall folding kinetics were observed in the time range of stopped-flow device, the contribution of residues to the formation of the each states occurred during the protein folding process can be investigated by applying folding kinetics measurements in conjunction with protein engineering using HubWA as a model protein.

Acknowledgments. Author appreciates Dr. Myeong-Hee Yu and Dr. Cheolju Lee in Korea Institute of Science and Technology for providing stopped-flow fluorescence spectrometer. Author also appreciates Dr. Heinrich Roder for providing human ubiquitin gene. This work was supported by the grant from Gangneung-Wonju National University in 2009.

References

1. Matouschek, A.; Kellis, J. T., Jr.; Serrano, L.; Fersht, A. R. *Nature* **1989**, *340*, 122.
2. Guydosh, N. R.; Fersht, A. R. In *Protein Folding Handbook, Part 1*; Keifhaber, T., Buchner, J., Eds.; Wiley-VCH: Weinhelm, Germany, 2005; p 445.
3. Zarrine-Afsar, A.; Davidson, A. R. *Methods* **2004**, *34*, 41.
4. Fersht, A. R. *Curr. Opin. Struct. Biol.* **1995**, *5*, 79.
5. Matouschek, A.; Kellis, J. T. J.; Serrano, L.; Bycroft, M.; Fersht, A. R. *Nature* **1990**, *346*, 440.
6. Itzhaki, L. S.; Otzen, D. E.; Fersht, A. R. *J. Mol. Biol.* **1995**, *254*, 260.
7. Lindorff-Larsen, K.; Vendruscolo, M.; Paci, E.; Dobson, C. M. *Nat. Struct. & Mol. Biol.* **2004**, *11*, 443.
8. Martinez, J. C.; Serrano, L. *Nat. Struct. Biol.* **1999**, *6*, (1010-1016).
9. Northey, J. G. B.; Di Nardo, A. A.; Davidson, A. R. *Nat. Struct. Biol.* **2002**, *9*, 126.
10. Riddle, D. S.; Grantcharova, V. P.; Santiago, J. V.; Alm, E.; Ruczincski, I.; Baker, D. *Nat. Struct. Biol.* **1999**, *6*, 1016.
11. McCallister, E. L.; Alm, E.; Baker, D. *Nat. Struct. Biol.* **2000**, *7*, 669.
12. Kim, D. E.; Fisher, C.; Baker, D. *J. Mol. Biol.* **2000**, *298*, 971.
13. Kragelund, B. B.; Osmark, P.; Neergaard, T. B.; Schiodt, J.; Kristiansen, K.; Knudsen, J.; Poulsen, F. M. *Nat. Struct. Biol.* **1999**, *6*, 594.
14. Khorasanizadeh, S.; Peters, I. D.; Butt, T. R.; Roder, H. *Biochemistry* **1993**, *32*, 7054.
15. Jackson, S. E. *Org. Biomol. Chem.* **2006**, *4*, 1845.
16. Khorasanizadeh, S.; Peters, I. D.; Roder, H. *Nat. Struct. Biol.* **1996**, *3*(2), 193.
17. Krantz, B. A.; Sosnick, T. R. *Biochemistry* **2000**, *39*, 11696.
18. Went, H. M.; Benitez-Cordoza, C. G.; Jackson, S. E. *FEBS Lett.* **2004**, *567*, 333.
19. Silow, M.; Oliveberg, M. *Proc. Natl. Acad. Sci. USA* **1997**, *94*, 6084.
20. Park, S.-H. *BMB Reports* **2008**, *41*, 35.
21. Peterman, B. F. *Anal. Biochem.* **1979**, *93*, 442.
22. Bachmann, A.; Kiefhaber, T. In *Protein Folding Handbook, Part I*; Buchner, J., Kiefhaber, T., Eds.; WILEY-VCH: Weinheim, Germany, 2005; p 379.
23. Tanford, C. *Adv. Prot. Chem.* **1970**, *24*, 1.
24. Chen, B.; Baase, W. A.; Schellman, J. A. *Biochemistry* **1989**, *28*, 691.
25. Matthews, C. R. *Methods Enzymol.* **1987**, *154*, 498.
26. Maxwell, K. L.; Wildes, D.; Zarrine-Afsar, A.; De Los Rios, M. A.; Brown, A. G.; Friel, C. T.; Hedberg, L.; Horng, J.-C.; Bona, D.; Miller, E. J.; Vallee-Belisle, A.; Main, E. R. G.; Bemporad, F.; Qiu, L.; Teilum, K.; Vu, N.-D.; Edwards, A. M.; Ruczinski, I.; Poulsen, F. M.; Kragelund, B. B.; Michnick, S. W.; Chiti, F.; Bai, Y.; Hagen, S. J.; Serrano, L.; Oliveberg, M.; Raleigh, D. P.; Wittung-Stafshede, P.; Radford, S. E.; Jackson, S. E.; Sosnick, T. R.; Marqusee, S.; Davidson, A.; Plaxco, K. W. *Protein Sci.* **2005**, *14*, 602.
27. Park, S.-H. *Bull. Korean Chem. Soc.* **2009**, *30*, 1567.
28. Baldwin, R. L. *Fold. Des.* **1996**, *1*, R1.
29. Wirmer, J.; Peti, W.; Schwalbe, H. *J. Biomol. NMR* **2006**, *35*, 175.
30. Kim, P. S.; Baldwin, R. L. *Annu. Rev. Biochem.* **1982**, *51*, 459.
31. Kim, P. S.; Baldwin, R. L. *Annu. Rev. Biochem.* **1990**, *59*, 631.
32. Park, S.-H.; O'Neil, K. T.; Roder, H. *Biochemistry* **1997**, *36*, 14277.